J. Indian Chem. Soc.,
Vol. 97, May 2020, pp. 753-759

Comparative DFT analysis of ELF topology and global properties of allyl and allenyl type three atom components (TACs)

Nivedita Acharjee*[a], Avijit Banerji[b], Mira Jhawar[a] and Ambar Barman[a]

[a]Department of Chemistry, Durgapur Government College, J. N. Avenue, Durgapur-713 214, West Bengal, India

E-mail: nivchem@gmail.com

[b]Central Ayurveda Research Institute for Drug Development, CN Block, Sector V, Kolkata-700 091, India

Manuscript received online 09 December 2019, revised and accepted 09 January 2020

The term three atom components (TACs) is used in molecular electron density theory to denote three centre four electron π systems, which react with multiple bonded compounds to generate stereo- and regiochemically defined five membered heterocycles by [3+2] cycloaddition reactions. TACs can be allyl type or allenyl type, and the electronic distribution of TACs is a crucial factor to dictate their selectivity and reactivity in [3+2] cycloaddition reactions. Electron localization function (ELF) topological analysis of the TACs have been compared and analyzed at DFT/B3LYP/6-311G(d,p) level of theory to get a precise idea of the proposed Lewis bonding model and reactivity of the TACs. This follows the classification of 12 different TACs as *pseudodiradical*, *pseudo(mono)radical*, carbenoid and *zwitter-ionic* type and analysis of the DFT based reactivity indices of the TACs.

Keywords: TAC, electron localization function, basins, DFT.

Introduction

Five membered heterocycles serve as versatile synthetic intermediates[1–3] and show potent biological significance[4]. The synthesis of five membered heterocycles containing multiple stereogenic centers is carried out by [3+2] cycloaddition reactions (32CAs) between two reactants. One of the reactants is a multiple bonded compound. The other reactant of 32CAs is an allyl-type or a propargyl/allenyl-type structure in which four electrons are shared in the π-system over three atoms. This reactant of 32CAs was termed as "1,3-dipole" since late 1880s and gained sincere attention due to the pharmaceutical importance of five-membered heterocycles. We can draw resonance structures of a 1,3-dipole to allow delocalization of positive and negative charges along the two ends. However, one can achieve at an accurate electronic distribution of the 1,3-dipole by using computational chemistry calculations.

In the 1960s, Fukui[5] proposed frontier molecular orbital theory (FMO) to explain the reactivity of 1,3-dipoles, which was subsequently followed by semi-empirical computational studies of the FMOs of 1,3-dipoles by Houk *et al.*[6] in 1973. Conceptual density functional theory (CDFT) was reviewed in 2003 by Geerlings *et al.*[7]. Subsequently, CDFT studies were employed to understand the electronic framework of 1,3-dipoles. Domingo *et al.*[8] proposed global electrophilicity scale in 2012 for different dienes and dienophiles from CDFT studies. In 2016, the term "1,3-dipole" was modified to "Three atom component (TAC)" after the advent of molecular electron density theory (MEDT) proposed by Domingo[9] in 2016. MEDT[9,10] focuses on the calculation of CDFT indices and Electron Localization Function (ELF) topology of these three atom components to unravel the mechanism of 32CA reactions in terms of activation energy calculations and following the reaction pathways by calculations of ELF basin populations[10].

DFT studies related to the optimization and ELF studies of TACs have been reported at the calculation levels requiring high computational cost and long run time. In this context, precision of a computationally effective calculation system is worth investigating, which is expected to reduce the run time and computational energies required for such calculations. With this in mind, the present study was carried

out for 12 TACs; nitrile ylide (**1**), nitrile imine (**2**), nitrile oxide (**3**), diazoalkene (**4**), azide (**5**), nitrous oxide (**6**), azomethine ylide (**7**), azomethine imine (**8**), nitrone (**9**), carbonyl ylide (**10**), carbonyl imine (**11**) and carbonyl oxide (**12**) at DFT/B3LYP/6-311G(d,p) level of theory to provide a complete rationalization of ELF topology and global properties of TACs. This calculation can be performed with the help of a simple i3 personal computer processor. This study is intended to provide a detailed comprehension of the classification, electronic distribution and global properties of the TACs. Lewis structures of the TACs have been proposed on the basis of the calculated electron densities at the ELF valence basins, and were found be in accordance to the communications reported at other higher computational levels under molecular electron density theory[9,10].

Computational methods:

Optimization of the TACs was performed at B3LYP/6-311G(d,p)[11,12] level of theory. Stationary states were identified by the absence of imaginary frequencies. The electronic chemical potential μ[8] and chemical hardness η[8,13] have been calculated from the computed HOMO and LUMO energies. The global electrophilicity index ω[8] is calculated using eq. (3).

$$\mu \approx 1/2\,[E_{HOMO} + E_{LUMO}] \quad (1)$$

$$\eta \approx E_{LUMO} - E_{HOMO} \quad (2)$$

$$\omega = \mu^2/2\eta \quad (3)$$

ELF topology of the TACs was calculated from Multiwfn (Version 3.6) software[14]. ELF basin analysis was performed with high quality grid with spacing 0.06 Bohr. ELF attractor images were visualized using VMD software[15] and UCSF Chimera software[16]. The calculations were performed using Gaussian 2003[17] set of programs along with the graphical interface Gauss View 2003.

Results and discussion

ELF topological analysis of the TACs:

Electron Localization Function (ELF) for atomic and molecular systems was introduced by Becke and Edgecombe[18] and the use of ELF attractors was outlined in a 1994 study[19] published in *Nature*. ELF attractors identify the core, bonding and non-bonding regions of a chemical system. A basin contains a whole region of points in space. One reaches at the attractor through steepest ascent along these points. We obtain a non-overlapping partition of the space through a basin calculation. MEDT[9] requires the ELF topological analysis of the TACs and calculation of ELF basin populations along the reaction pathway provides a precise idea of the plausible reaction mechanism. ELF topological analysis classifies TACs into *pseudodiradical* type (pdr-type), *pseudo (mono) radical* type (pmr-type), carbenoid type (cb-type) and *zwitter-ionic* type (zw-type)[9,10]. ELF topology of TACs has been employed to study 32CA reactions of nitrile ylides[20], azomethine ylide[20], nitrile imine[21], azomethine imine[22], nitrone[23] and nitrile oxide[24].

B3LYP/6-311G(d.p) level of theory is an appropriate system of calculation with respect to computational cost. Hence, the precision and accuracy of this system of calculation is worth investigating to underline its applicability for TAC optimizations and analysis. With this in mind, the present study deals with the ELF topological analysis of 12 TACs at B3LYP/6-311G(d.p), level of theory and aims to investigate the precision of this level of theory to identify the classification and reactivity of the TACs: nitrile ylide (**1**), nitrile imine (**2**), nitrile oxide (**3**), diazoalkane (**4**), azide (**5**), nitrous oxide (**6**), azomethine ylide (**7**), azomethine imine (**8**), nitrone (**9**), carbonyl ylide (**10**), carbonyl imine (**11**) and carbonyl oxide (**12**). Fig. 1 shows the ELF attractor positions at B3LYP/6-311G(d,p) level of theory of the investigated TAC series. TACs can be classified from the total integrating populations of the ELF valence basins[9,10,20].

Monosynaptic basins integrating at less than 1e are associated with pseudoradical centers. TACs which show the presence of two pseudoradical centers are classified as *pseudodiradical* type[20] (pdr) TACs, while those with one pseudoradical centre are classified as *pseudo(mono)radical* type[22] (pmr) TACs. Monosynaptic basins integrating at 2e in neutral molecules are associated with carbenoid centers and the TACs with carbenoid centre are classified as carbenoid type[20] (cb-) TACs. Absence of any pseudoradical or carbenoid centre in the TACs classifies them as *zwitter-ionic* type (zw) TAC[23,24]. The reactivity of TACs follows the order: *pseudodiradical* type > carbenoid type > *zwitter-ionic* type[8,9].

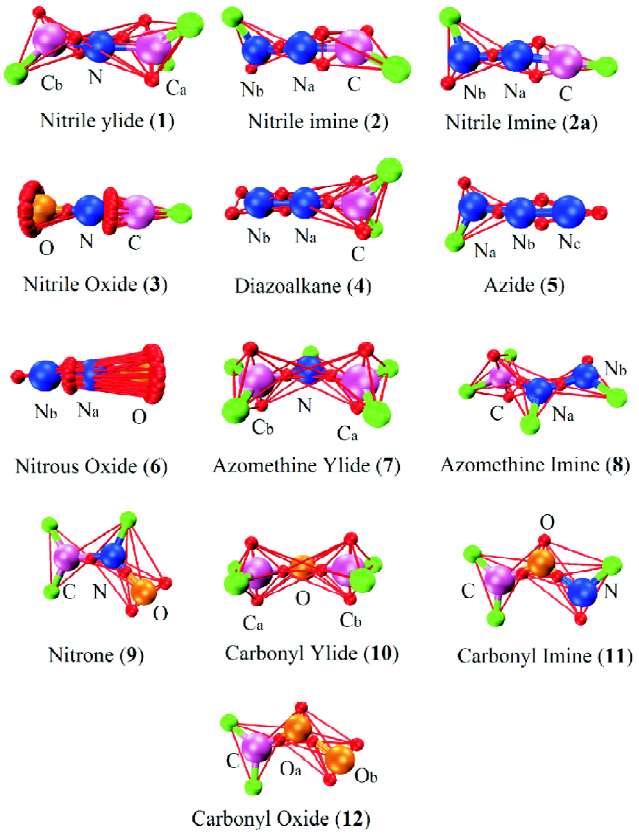

Fig. 1. DFT/B3LYP/6-311G(d,p) calculated ELF attractor positions of the TACs. Red spheres indicate ELF attractor positions. Green spheres indicate hydrogen atoms, pink spheres indicate carbon atoms, blue spheres indicate nitrogen atoms and yellow spheres indicate oxygen atoms (Attractor positions for hydrogen atoms are omitted to avoid complexity).

ELF attractor positions in the TACs are shown as red spheres in Fig. 1. The ELF valence basin populations of the investigated TACs are listed in Table 1. Red spheres on an atom are associated with the non-bonding electron density, while red spheres between two atoms indicate the bonding attractor positions.

In nitrile ylide **1**, we observe one red sphere on carbon atom Cb, which can be associated with carbenoid or pseudoradical centre depending on its ELF valence basin population. Nitrile ylide (**1**) shows the presence of one monosynaptic basin at Cb integrating at 1.89e, which can be associated with a carbenoid centre (see Table 1). Hence **1** can be classified as cb-type TAC. This is in complete agreement with the carbenoid classification of **1** at other levels of theory[20]. Two red spheres between Cb and N are the bonding attractor positions for the Cb-N double bond integrating at 4e (see Table 1), while one red sphere between Ca and N is the bonding attractor position for the underpopulated Ca-N double bond integrating at 3e (see Table 1).

In case of nitrile imine, we obtained two optimized structures **2** and **2a**. Nitrile imine **2** shows a carbenoid centre at the carbon atom (see red sphere on C in Fig. 1) integrating at 1.64e, thus allowing its classification as cb-type TAC. On the other hand, another optimized structure **2a** shows two red spheres between C and Na associated with bonding attractor for the C-Na overpopulated double bond integrating at 4.80e (see Table 1) and one red sphere between Na and Nb for the overpopulated single bond integrating at 2.21e (see Table 1). One red sphere on Nb indicates the attractor position for non-bonding electron density on Nb integrating at 3.54e (see Table 1). Thus, **2a** allows zw type classification due to absence of any pseudoradical or carbenoid centre. This is in complete agreement with the reported studies of Domingo *et al.*[21] and Begue *et al.*[25], where nitrile imine shows allenic geometry **2** and propargylic geometry **2a** is a transition state in between two allenic geometries of nitrile imine.

Similarly, nitrile oxide (**3**), azide (**5**), nitrous oxide (**6**), nitrone (**9**), carbonyl imine (**11**) and carbonyl oxide (**12**) do not show the presence of pseudoradical or carbenoid centre and hence can be classified as zw-type TACs. In these TACs, we find red spheres as bonding attractors between atoms as well as for attractor positions associated with non-bonding electron density on oxygen and nitrogen atoms.

In, diazoalkane **4**, we observe two red spheres on the carbon atom (see Fig. 1), indicating the ELF attractor position for the pseudoradical centre at carbon integrating at 0.96e (see Table 1), which allows its classification as pmr-type TAC.

The two symmetrical TACs, azomethine ylide (**7**) and carbonyl ylide (**10**), show the presence of two red spheres each on the carbon atoms Ca and Cb (Fig. 1), which are associated with the pseudoradical centers integrating at 0.84e and 0.82e respectively (Table 1) and hence can be classified as pdr-type TAC.

In azomethine imine, **8**, we find two red spheres on carbon atom associated with the presence of pseudoradical

Table 1. DFT/B3LYP/6-311G(d,p) calculated ELF basin populations of the TACs (Numbering of the atoms in TACs refer to that of Fig. 1)

TAC	ELF valence basins and their calculated total integrating populations										
1	V(Cb)	V(Cb-H)	V(Ca)	V(Ca)	V(Cb-N)	V(Cb-N)	V(Ca-N)	V(Ca-H)	V(Ca-H)		
	1.89	1.96	0.27	0.22	2.00	2.00	3.00	2.18	2.17		
2	V(Nb)	V(Nb-H)	V(C)	V(C-H)	V(C-Na)	V(C-Na)	V(Na-Nb)				
	3.29	1.93	1.64	2.07	2.31	2.16	2.28				
2a	V(Nb)	V(Nb-H)	V(C)	V(C-H)	V(C-Na)	V(C-Na)	V(Na-Nb)				
	3.54	1.88	–	3.26	2.66	2.14	2.21				
3	V(C-H)	V(C-N)	V(N-O)	V(O)							
	2.57	5.79	1.66	5.64							
4	V(C-H)	V(Na-Nb)	V(Na-Nb)	V(C-Na)	V(Nb)	V(Nb)	V(C-H)	V(C)	V(C)		
	2.10	1.82	1.82	3.05	1.92	1.92	2.10	0.48	0.48		
5	V(Nc)	V(Nb-Nc)	V(Na-Nb)	V(Na)	V(Nb-Nc)	V(Na-H)					
	3.82	2.48	2.39	3.45	1.66	1.88					
6	V(O)	V(Nb) +V(Na-Nb)	V(Na-O)	V(Na-Nb)							
	5.57	4.57	1.73	3.79							
7	V(Ca-H)	V(Ca-H)	V(Ca)	V(Ca)	V(Cb)	V(Cb)	V(N-H)	V(Ca-N)	V(Cb-H)	V(Cb-H)	
	2.19	2.17	0.42	0.42	0.420	0.42	2.15	2.58	2.17	2.19	
8	V(Nb)	V(C)	V(C)	V(Nb-H)	V(C-H)	V(C-H)	V(C-Na)	V(Na-Nb)	V(Na-H)		
	3.51	0.29	0.29	1.98	2.19	2.21	3.02	1.96	2.21		
9	V(C-H)	V(O)	V(O)	V(C-H)	V(C-N)	V(N-O)	V(N-H)				
	2.20	2.83	3.01	2.21	3.71	1.45	2.26				
10	V(Ca-H)	V(Ca-H)	V(Ca)	V(Ca)	V(O)	V(Ca-O)	V(Cb)	V(Cb)	V(O-Cb)	V(Cb-H)	V(Cb-H)
	2.25	2.19	0.41	0.41	3.07	2.03	0.41	0.41	2.03	2.25	2.19
11	V(C-H)	V(O)	V(C-O)	V(N-H)	V(N)	V(C-H)	V(N-O)				
	2.74	3.31	2.30	2.00	3.69	2.26	1.38				
12	V(Ob)	V(Oa)	V(Ob)	V(C-Oa)	V(C-H)	V(C-H)	V(Oa-Ob)				
	3.11	3.38	2.91	2.70	2.29	2.25	1.03				

centre integrating at 0.58e and hence **8** can be classified as pmr type TAC, which agrees well with its classification reported at different levels of theory[22]. In azomethine imine, we also find red spheres as bonding attractor positions between Na-Nb and C-Na, along with red sphere on nitrogen atom Nb associated with the lone pair electron density integrating at 3.51e (see Table 1).

Fig. 2 shows the ELF localization domains of the investigated TACs, where monosynaptic, disynaptic, proton and core basins are shown in different colours. Basins are identified as monosynaptic and disynaptic respectively being participated by one and two atomic valence shells.

The proposed Lewis bonding model of the TACs on the basis of ELF basin populations is represented in Fig. 3. Monosynaptic basins V(A) are associated with lone pairs of the Lewis bonding model. The shared pair of electrons in the Lewis bonding model are denoted by the presence of polysynaptic basins.

ELF valence disynaptic basins with the total integrating populations approximately closer to 2e, 4e and 6e are indicated by the single, double and triple bonds between the respective atoms. The pseudoradical centres integrating at less than 1e are present in diazoalkane (**4**), azomethine ylide (**7**), azomethine imine (**8**) and carbonyl ylide (**10**). Carbenoid centres integrating at about 2e are shown in nitrile ylide (**1**) and nitrile imine (**2**).

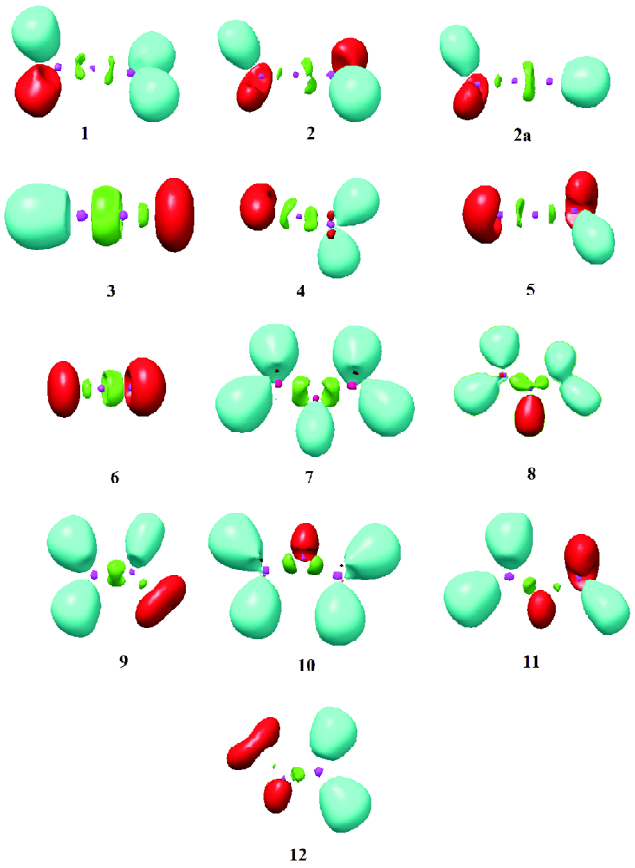

Fig. 2. ELF localization domains [Isovalue: 0.79] of the TACs. Protonated basins are shown in blue, disynaptic basins are shown in green, monosynaptic basins are shown in red and core basins are shown in magenta colours.

Analysis of FMOs and global properties:

Table 2 lists the DFT/B3LYP/6-311G(d,p) calculated frontier molecular orbital (FMO) energies and CDFT indices, electronic chemical potential, μ, global hardness, η, and global electrophilicity, ω of the investigated series of TACs. Now, let us divide the investigated TAC series into four fragments, [**1-3**], [**4-6**], [**7-9**] and [**10-12**]. In each fragment of the investigated series, change of one atom leads to two TACs of the same fragment. For example, carbon in nitrile ylide (**1**) is changed to nitrogen in nitrile imine (**2**) and to oxygen in nitrile oxide (**3**), keeping the other two atoms unaltered and the allyl/allenyl system. As we move along the series from nitrile ylide (**1**) to nitrile imine (**2**) and then to nitrile oxide (**3**), there is increase in the HOMO-LUMO energy gap. This increase in the FMO energy gap is also observed as we move from diazomethane (**4**) to nitrous oxide (**6**), from azomethine ylide (**7**) to nitrone (**9**) and from carbonyl ylide (**10**) to carbonyl oxide (**12**). If we consider the TAC classification, then moving from **1** to **2** to **3** leads to the change in TAC type from cb-type in **1** and **2** to zw-type in **3**. Now, reactivity of cb-type TAC is higher than zw-type TAC, which is reflected in the increase in FMO energy gap from **1** to **3**. Similarly, change in TAC from pmr-type in **4** to zw-type in **6**, from pdr-type in **7** to pmr-type in **8** and zw-type in **9**, from pdr-type in **10** to zw-type in **12** leads to increase in the HOMO-LUMO energy gap, thus indicating the decrease in reactivity of the TAC.

Along the four fragments of the series, the zw-type TACs show lowest values of electronic chemical potential, μ in each fragment, which reflects the decreased tendency of zw-type TACs to acquire electronic charge. Domingo[8,9] proposed the electrophilicity scale to classify organic molecules according to their global electrophilicity, ω. Molecules with ω > 1.5 eV are strong electrophiles, moderate electrophiles show 0.8 eV < ω < 1.5 eV and marginal electrophiles show ω < 0.8 eV. For the present study, **1, 2, 3, 5, 6, 8, 9** and **10** can be classified as a moderate electrophile with 0.8 eV < ω < 1.5 eV. **4** (ω = 1.49 eV) can be classified in the borderline of moderate and strong electrophiles. Azomethine ylide, **7** (ω = 0.55 eV) is a marginal electrophile, while **11** (ω = 1.90 eV) and **12** (ω = 2.74 eV) can be classified as the strong electrophiles.

Table 2. DFT/B3LYP/6-311G(d,p) calculated global properties of the TACs

TAC	HOMO (eV)	LUMO (eV)	LUMO-HOMO (eV)	μ (eV)	η (eV)	ω (eV)
1	–5.82	–0.46	5.36	–3.14	5.36	0.92
2	–6.61	–0.71	5.90	–3.66	5.9	1.13
3	–7.59	0.24	7.84	–3.67	7.84	0.86
4	–6.18	–1.39	4.79	–3.78	4.79	1.49
5	–7.62	–0.98	6.64	–4.3	6.64	1.39
6	–9.44	–0.52	8.92	–4.98	8.92	1.39
7	–4.38	0.00	4.38	–2.19	4.38	0.55
8	–5.25	–0.44	4.82	–2.84	4.82	0.84
9	–6.42	–0.95	5.47	–3.69	5.47	1.24
10	–4.87	–1.14	3.73	–3.01	3.73	1.21
11	–5.80	–1.90	3.89	–3.85	3.89	1.90
12	–6.83	–2.69	4.14	–4.76	4.14	2.74

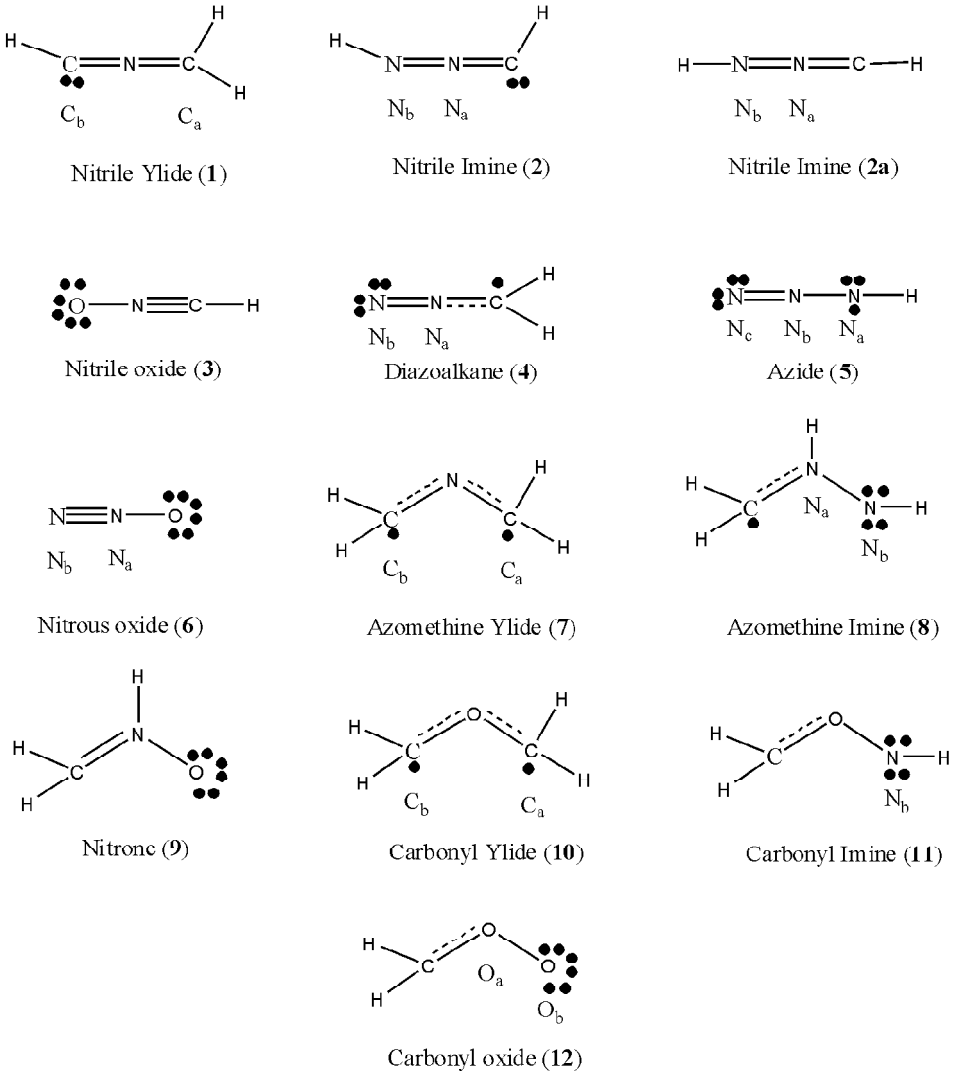

Fig. 3. Proposed Lewis bonding model of the TAC based on DFT/B3lYP/6-311G(d,p) calculated ELF valence basin populations.

Conclusion

B3LYP/6-311G(d,p) level of theory is a computationally effective process to study the classification and reactivity of TACs with good precision. The calculated ELF valence basin populations at this level of theory allowed correct classification of the TACs as carbenoid, *pseudodiradical*, *pseudo(mono)radical* or *zwitter-ionic* type. Consequently, Lewis bonding models of the TACs could be proposed on the basis of ELF topology of the TACs at this level of theory. Analysis of FMO energies were also found to be in complete agreement with the reactivity trend of the TACs.

References

1. H. Feuer and K. B. G. Torssell, "Nitrile Oxides, Nitrones and Nitronates in Organic Synthesis", 2nd ed., Wiley-International, New York, 2008.
2. A. Banerji and P. Sengupta, *J. Indian Inst. Sci.,* 2001, **81**, 313.
3. N. Acharjee, A. Banerji and B. Gayen, *J. Indian Chem. Soc.,* 2011, **88**, 1857.
4. J. T. Sharp, in: "The Chemistry of Heterocyclic Compounds Synthetic Applications of 1,3-Dipolar Cycloaddition Chemistry toward Heterocycles and Natural Products", eds. A. Padwa and W. H. Pearson, John Wiley & Sons, New York, 2002, p. 473.
5. K. Fukui, "Molecular orbitals in Chemistry, Physics and Biology",

eds. P.-O. Löwdin and B. Pullman, Academic Press, New York, 1964, p. 513.

6. K. N. Houk, J. Sims, R. E. Duke (Jr.), R. W. Strozier and J. K. George, *J. Am. Chem. Soc.*, 1973, **95**, 7287.
7. P. Geerlings, F. De Proft and W. Langenaeker, *Chem. Rev.,* 2003, **103**, 1793.
8. L. R. Domingo, M. J. Aurell, P. Pérez and R. Contreras, *Tetrahedron*, 2002, **58**, 4417.
9. L. R. Domingo, *Molecules,* 2016, **21**, 1319.
10. L. R. Domingo, M. R. Gutiérrez and P. Pérez, *Molecules*, 2016, **21**, 748.
11. R. G. Parr and W. Yang, "Density Functional Theory of Atoms and Molecules", Oxford University Press, New York, 1989.
12. J. T.-Rives and W. L. Jorgensen, *Chem. Theory Comput.,* 2008, **4**, 2297.
13. R. G. Parr and R. G. Pearson, *J. Am. Chem. Soc.*, 1983, **105**, 7512.
14. T. Lu and F. Chen, *J. Comput. Chem.*, 2012, **33**, 580.
15. W. Humphrey, A. Dalke and K. Schulten, *J. Molec. Graphics.*, 1996, **14**, 33.
16. E. F. Pettersen, T. D. Goddard, C. C. Huang, G. S. Couch, D. M. Greenblatt, E. C. Meng and T. E. Ferrin, *J. Comput. Chem.*, 2004, **25**, 1605.
17. Gaussian 03, Revision D.01, M. J. Frisch, G. W. Trucks, H. B. Schlegel, G. E. Scuseria, M. A. Robb, J. R. Cheeseman, J. A. Montgomery (Jr.), T. Vreven, K. N. Kudin, J. C. Burant, J. M. Millam, S. S. Iyengar, J. Tomasi, V. Barone, B. Mennucci, M. Cossi, G. Scalmani, N. Rega, G. A. Petersson, H. Nakatsuji, M. Hada, M. Ehara, K. Toyota, R. Fukuda, J. Hasegawa, M. Ishida, T. Nakajima, Y. Honda, O. Kitao, H. Nakai, M. Klene, X. Li, J. E. Knox, H. P. Hratchian, J. B. Cross, V. Bakken, C. Adamo, J. Jaramillo, R. Gomperts, R. E. Stratmann, O. Yazyev, A. J. Austin, R. Cammi, C. Pomelli, J. W. Ochterski, P. Y. Ayala, K. Morokuma, G. A. Voth, P. Salvador, J. J. Dannenberg, V. G. Zakrzewski, S. Dapprich, A. D. Daniels, M. C. Strain, O. Farkas, D. K. Malick, A. D. Rabuck, K. Raghavachari, J. B. Foresman, J. V. Ortiz, Q. Cui, A. G. Baboul, S. Clifford, J. Cioslowski, B. B. Stefanov, G. Liu, A. Liashenko, P. Piskorz, I. Komaromi, R. L. Martin, D. J. Fox, T. Keith, M. A. Al-Laham, C. Y. Peng, A. Nanayakkara, M. Challacombe, P. M. W. Gill, B. Johnson, W. Chen, M. W. Wong, C. Gonzalez and J. A. Pople, Gaussian, Inc., Wallingford CT, 2004.
18. A. D. Becke and K. E. Edgecombe, *J. Chem. Phys.*, 1990, **92**, 5397.
19. B. Silvi and A. Savin, *Nature*, 1994, **371**, 683.
20. L. R. Domingo, M. R. Gutiérrez and P. Pérez, *Tetrahedron*, 2016, **72**, 1524.
21. M. R. Gutiérrez and L. R. Domingo, *Tetrahedron*, 2019, **75**, 1961.
22. L. R. Domingo and M. R. Gutiérrez, *Molecules*, 2017, **22**, 750.
23. L. R. Domingo and N. Acharjee, *Chemistry Select*, 2018, **3**, 8373.
24. L. R. Domingo, M. R. Gutiérrez and N. Acharjee, *Molecules*, 2019, **24**, 832.
25. D. Begue and C. Wentrup, *J. Org. Chem.*, 2014, **79**, 1418.